

SPACE

TIME

+

MATTER

© 2001 CERN

Cosmological Parameters 2000

CMK 2001

## (i) HST - KEY PROJECT:

⇒ use Cepheid DISTANCES to 25 Galaxies within 25 Mpc  
 to calibrate secondary distance indicators : (1) Tully-Fisher relation  
 (spiral) (2) FUNDAMENTAL PLANE (Ellipticals), (3) SBF (luminosities) (4) SNIa

⇒ each of these then used to measure the:

$$\left. \begin{array}{l} H_{\text{TF}} = 71 \pm 4 \pm 7 \\ H_{\text{FPP}} = 78 \pm 8 \pm 10 \\ H_{\text{SFR}} = 69 \pm 4 \pm 6 \\ H_0^{\text{SNIa}} = 68 \pm 2 \pm 5 \end{array} \right\} \Rightarrow H_0 = 71 \pm 6 \text{ km s}^{-1} \text{ Mpc}^{-1} (1\sigma) \quad (\pm 8) \quad (97\% - 1\sigma)$$

↳ LMC-distance  
 (see fig)  
 (if Cepheid instability - 4%)  
 $\Rightarrow [68 \pm 6]$

## OTHER MEASURES:

(ii) S-Z Effect:  $\Sigma_c \rightarrow$  CMB photon scattering on clusters of matter  
 → shift to higher energy.

SZE → Sunyaev-Zel'dovich effect

Compton X-Ray Intensity  $\sim \int n_e^2 d\Omega$

$\Rightarrow \therefore$  the models  $\Rightarrow n_e, n_e^2 \rightarrow d\Omega \rightarrow$  physical Scale  $\Leftrightarrow$  angular size!  
 $\Rightarrow$  distance measure!  
 (assume  $d\Omega \perp \Rightarrow d\Omega_{\parallel\perp}$ )  $\therefore$  statistical.

# ① SPACE

⇒ EXPANSION RATE

⇒ GEOMETRY

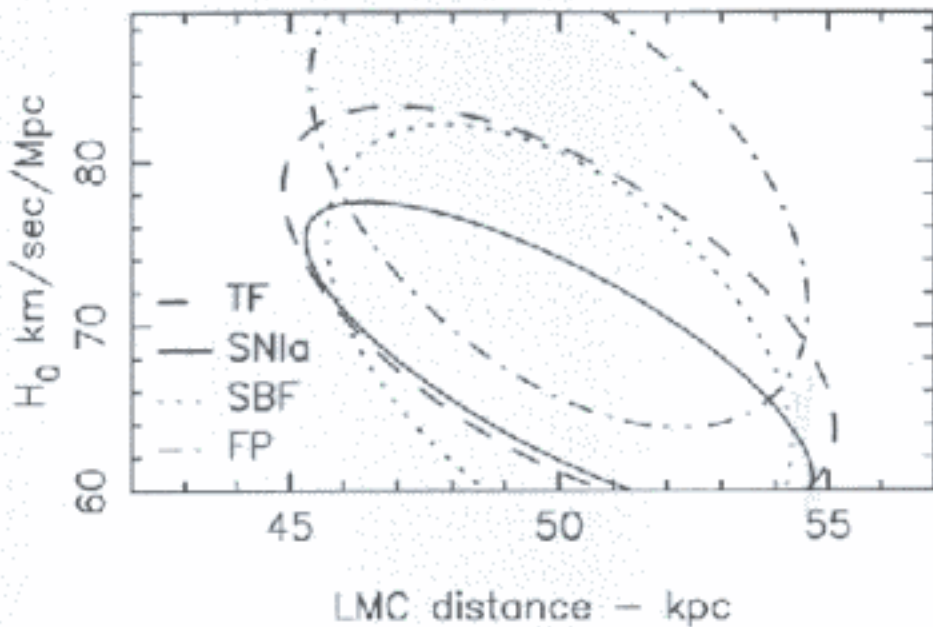
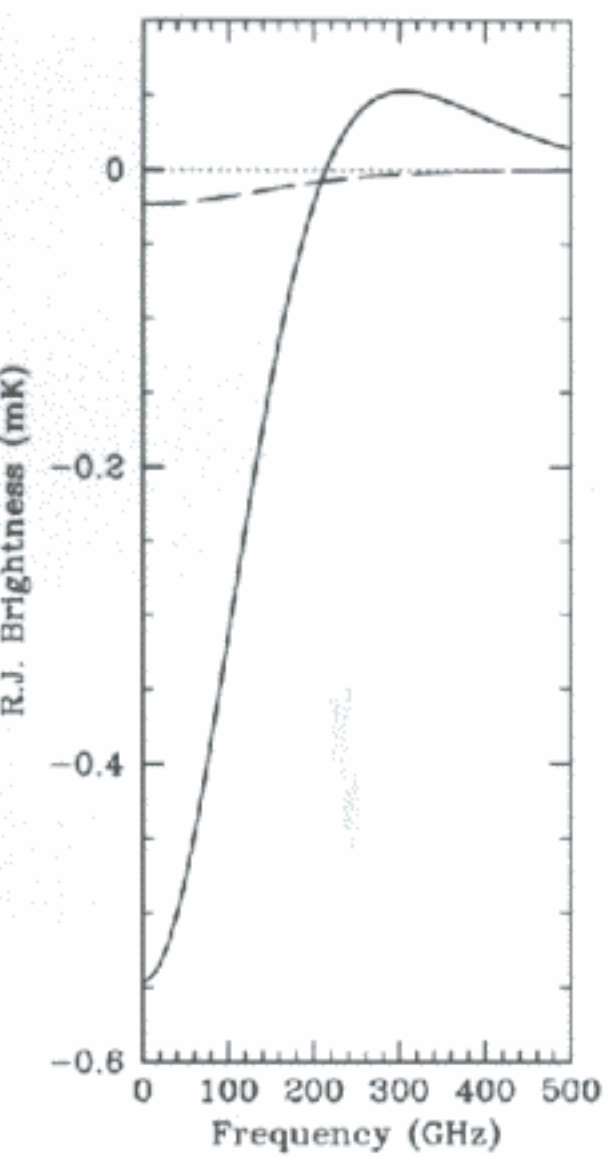
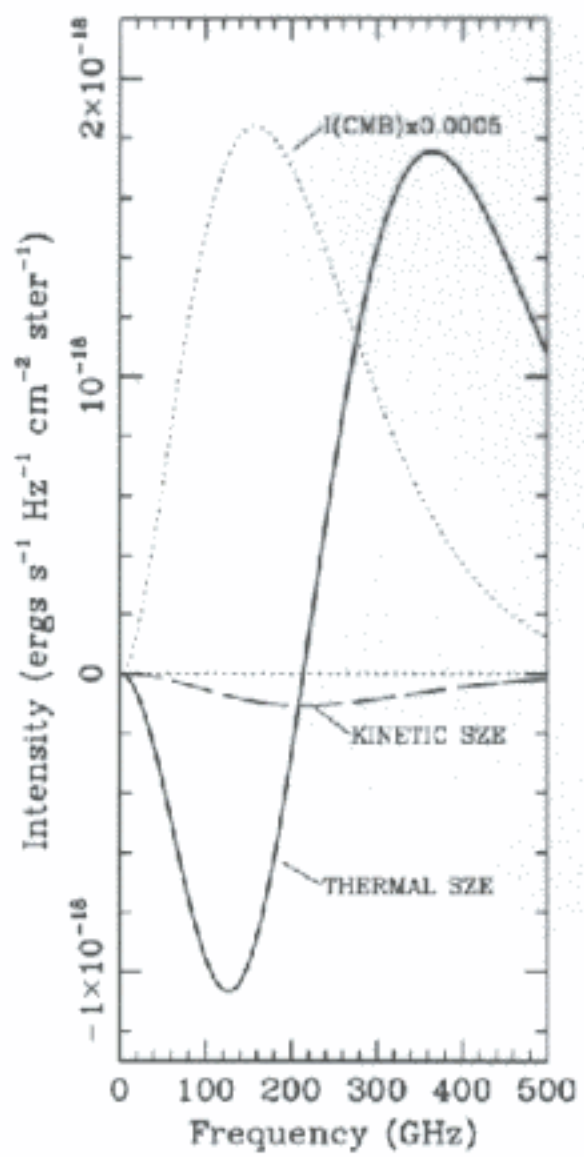
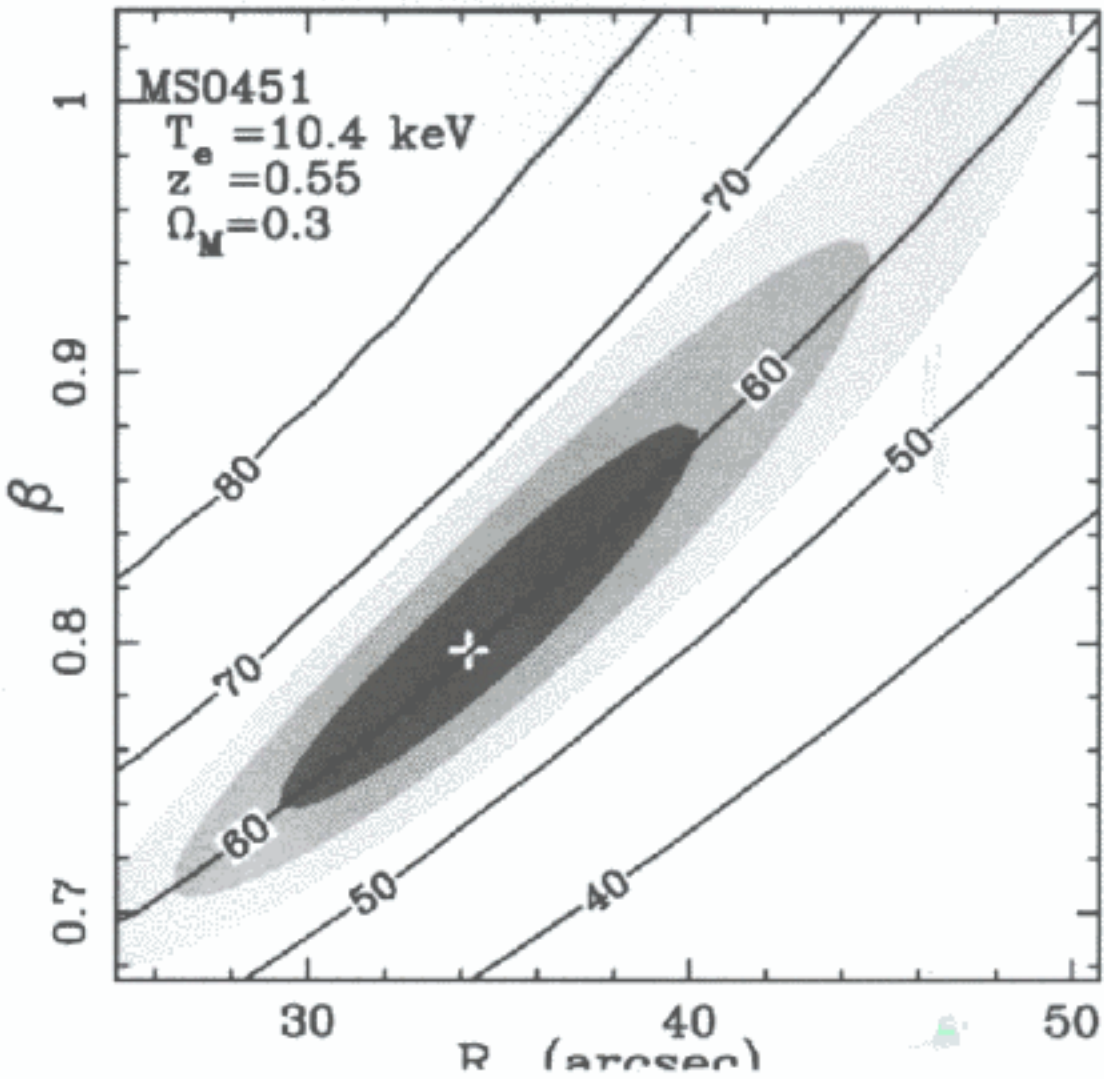


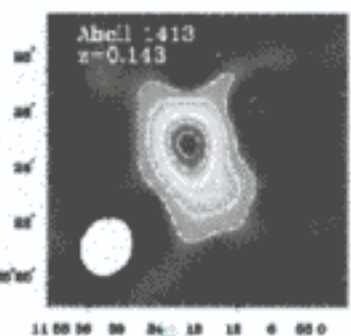
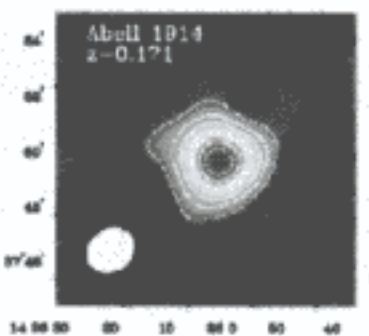
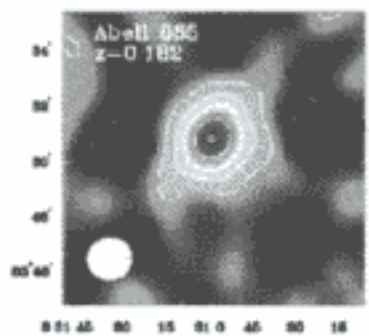
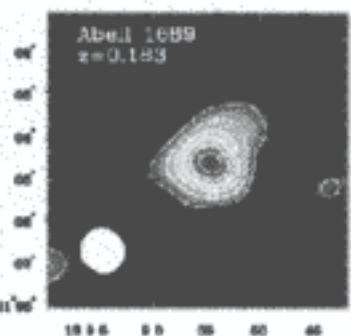
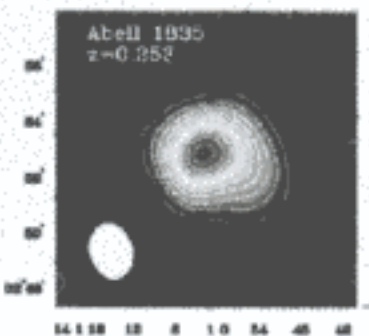
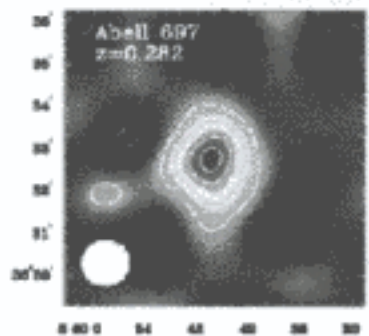
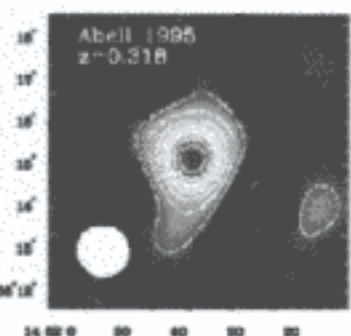
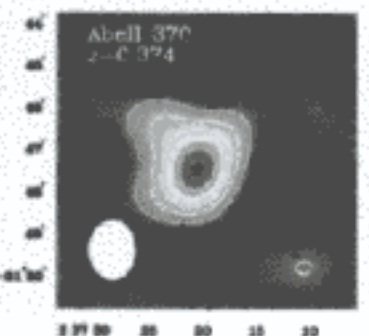
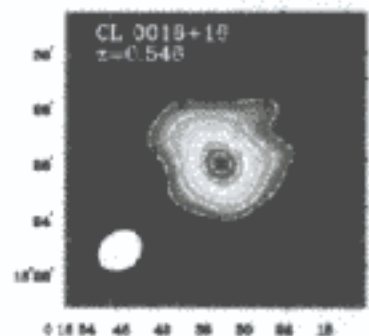
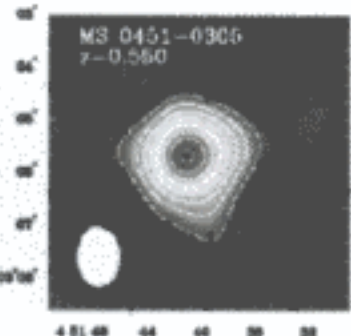
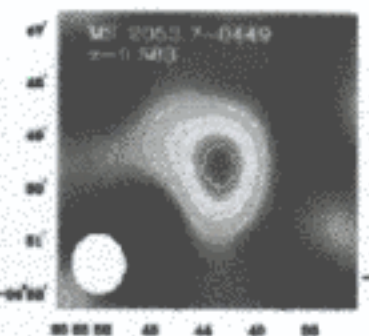
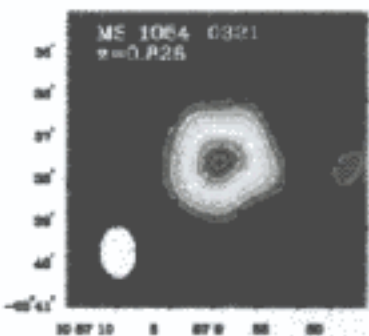
Fig. 5.— The Key Project calibration constrains  $H_0$  in four ways, but these are each, in turn, dependent on the assumed distance of the Large Magellanic Cloud which provides the reference Cepheid PL relation for the project.

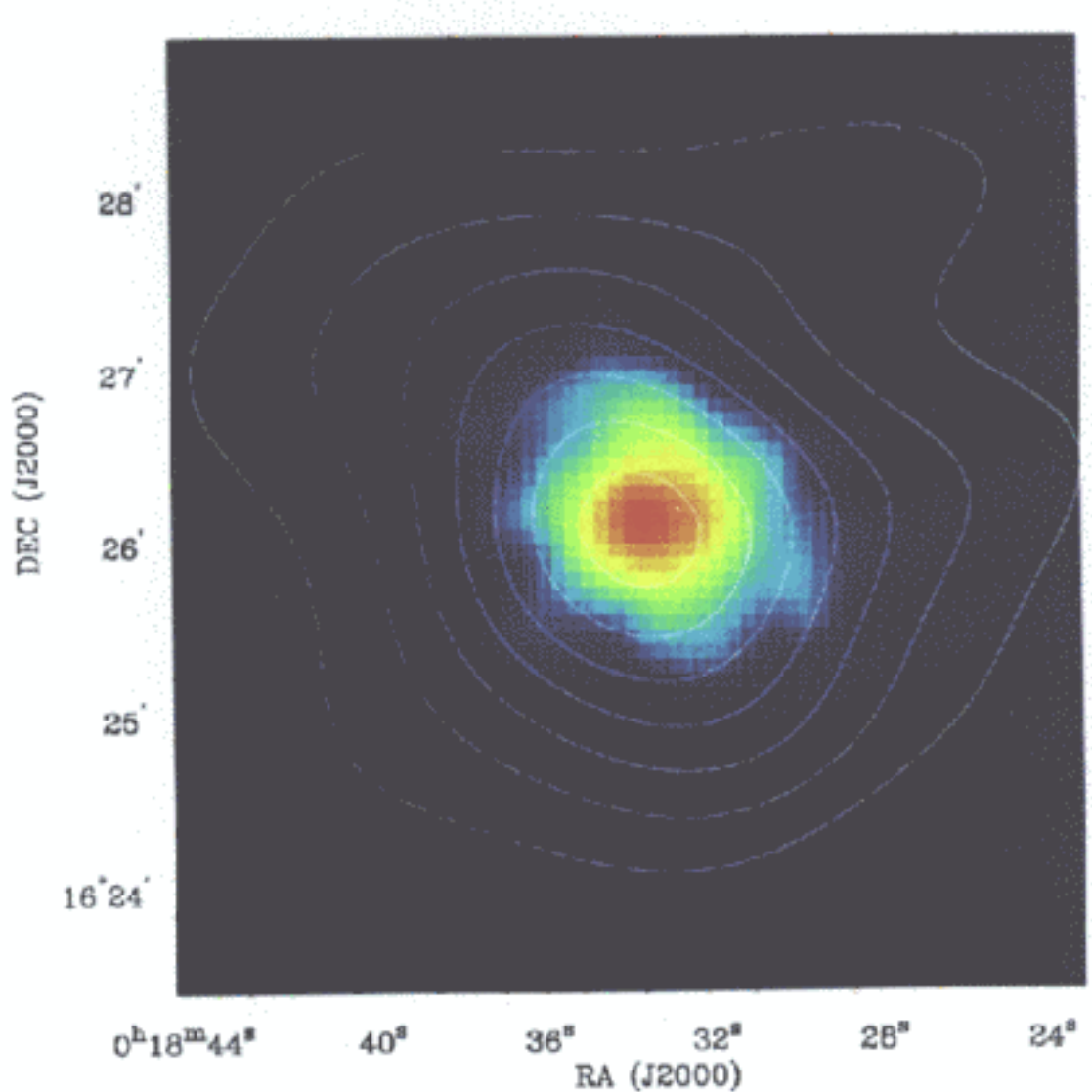


Journal of  
Plasma Physics

Volume 37 Number 1 February 2001







http://www.astronomy.org/references/astrophysics/astrophysics.html

(ii)  $H_0 = 60 \pm 10 \text{ km s}^{-1} \text{ Mpc}^{-1}$  SZE

(iii) Type Ia SN  $\Rightarrow$  (distant group)

$$H_0 = 64^{+8}_{-6} \text{ km s}^{-1} \text{ Mpc}$$

(iv) SBF - Galaxy Density Field

$$H_0 = 74 \pm 4 \text{ km s}^{-1} \text{ Mpc}^{-1}$$

(V) TIME-DELAY: GRAN. LENSING  $Q 0957 + 561$  ( $T_h = 417 \pm 38$ )

$$H_0 = 69^{+18}_{-12} (1-k) \text{ or } 74^{+18}_{-12} (1-k)$$

(k-cluster parameter)

AVERAGE =  $69.7 \pm 3.5 \text{ km s}^{-1} \text{ Mpc}^{-1}$

$$\Rightarrow H_0 \in \{63-77\} \text{ 99% CL}$$

## (B) GEOMETRY

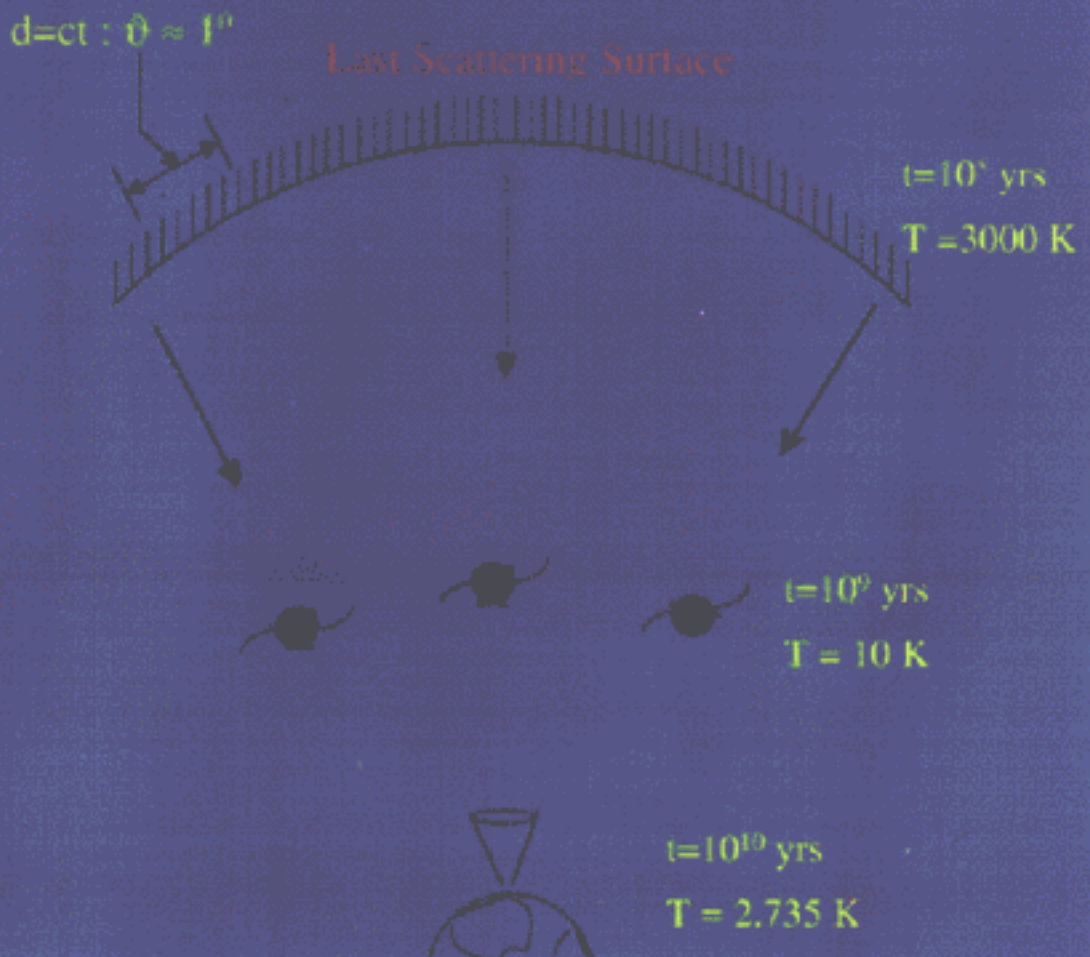
⇒ CMB: A FIDUCIAL LENGTH!

Note:

Traditionally:

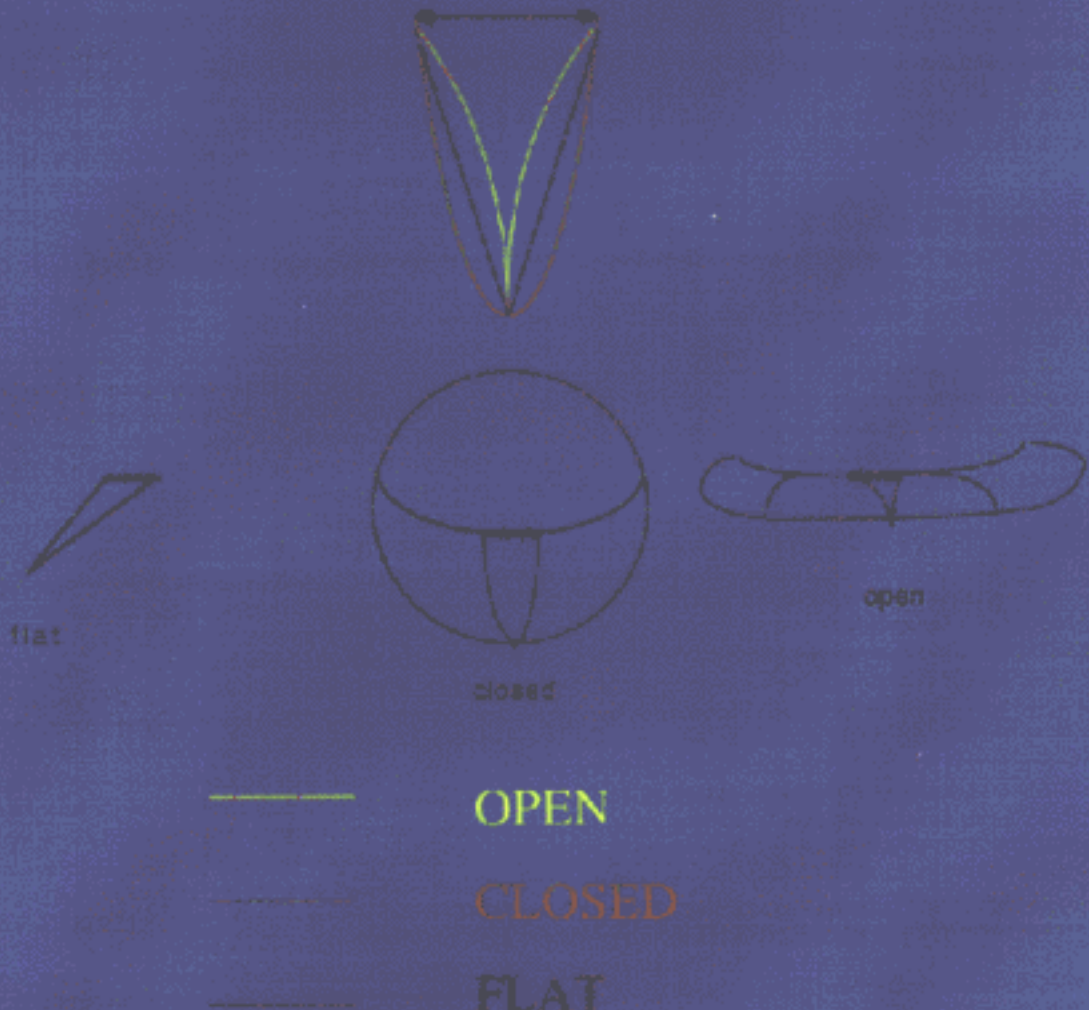
$$H^2 = \frac{8\pi G}{3} \rho + \frac{k}{R^2}$$

# COSMIC MICROWAVE BACKGROUND

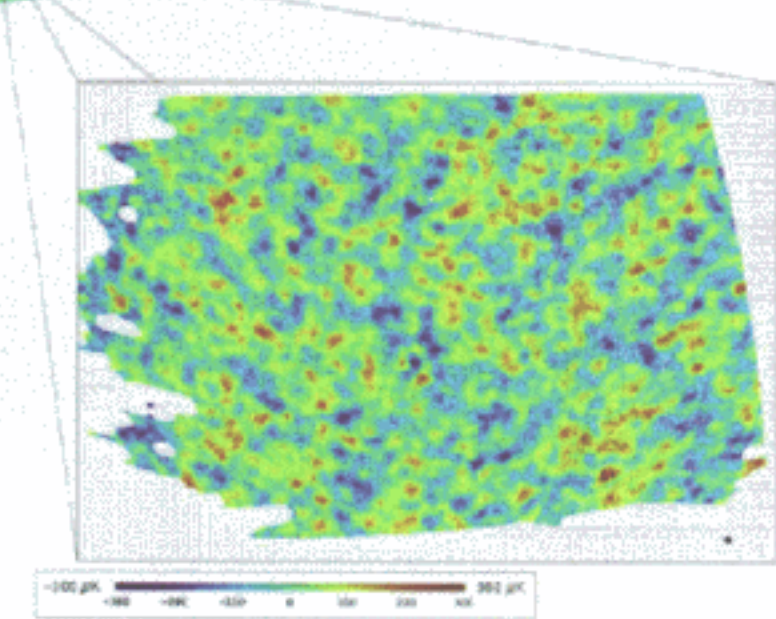
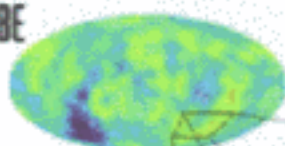


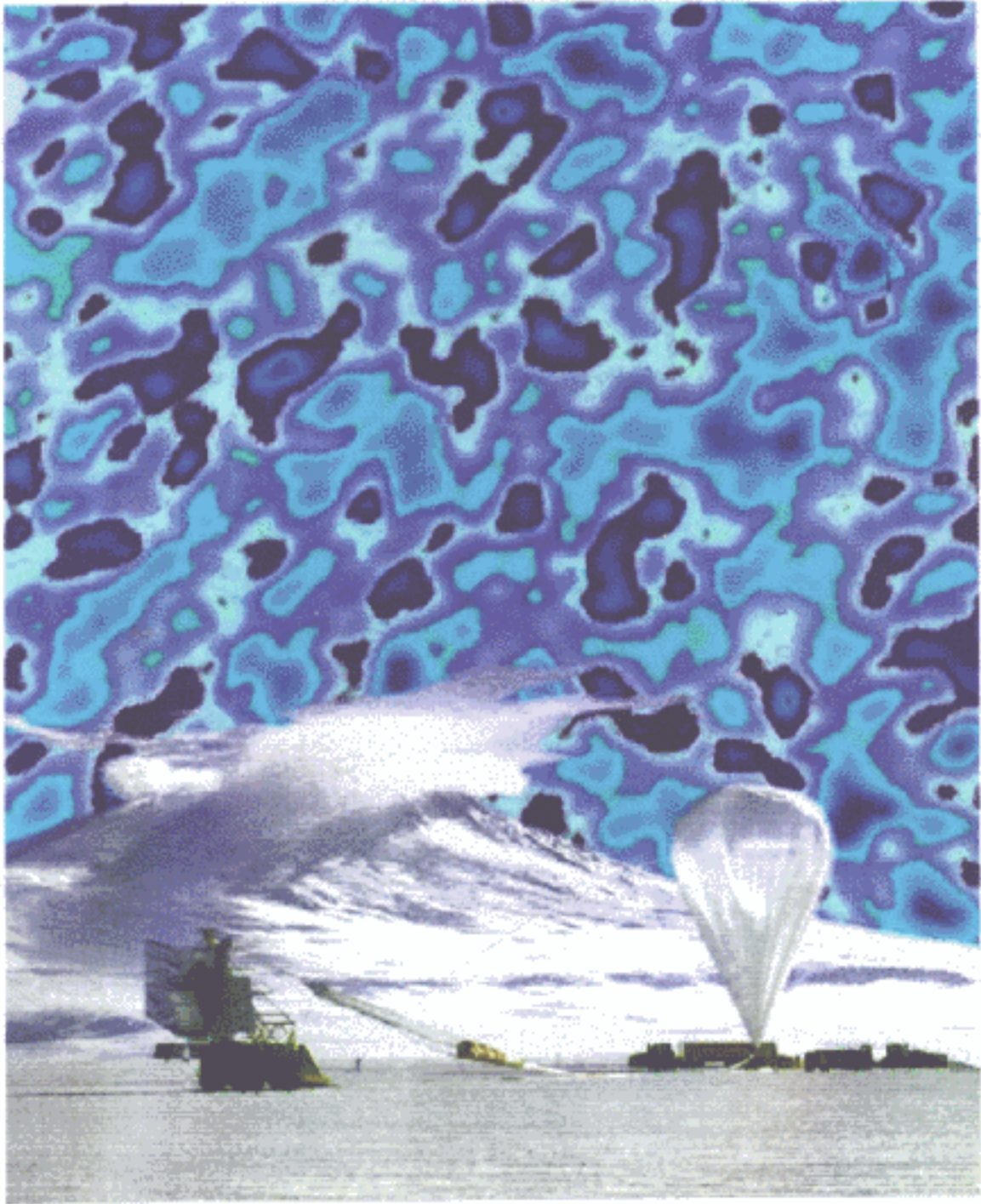
# Angular Size of a Fixed Scale in Open, Closed, and Flat Universes:

First Scale to Collapse after  
Recombination ( $\sim$ distance spanned  
by light ray =horizon size)

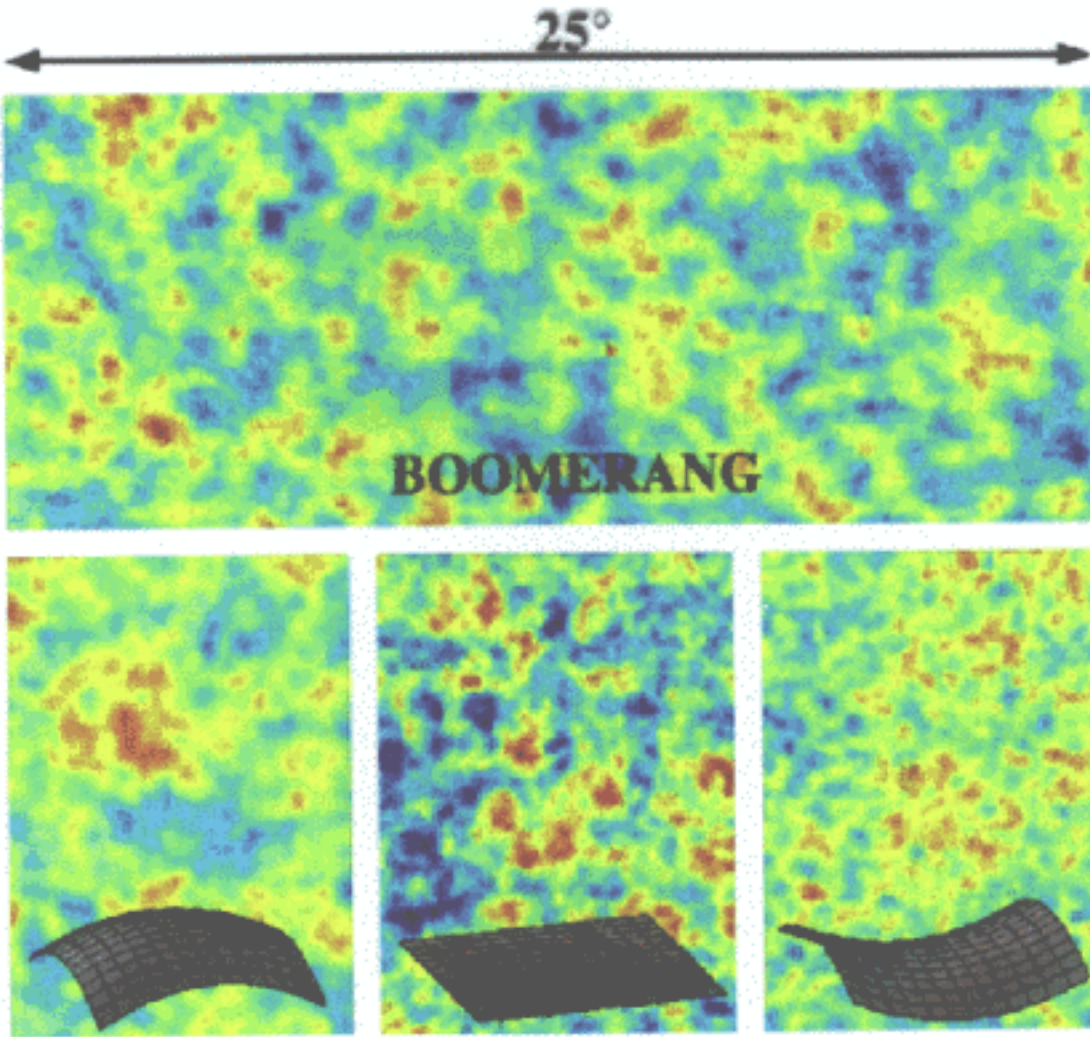


COBE





5



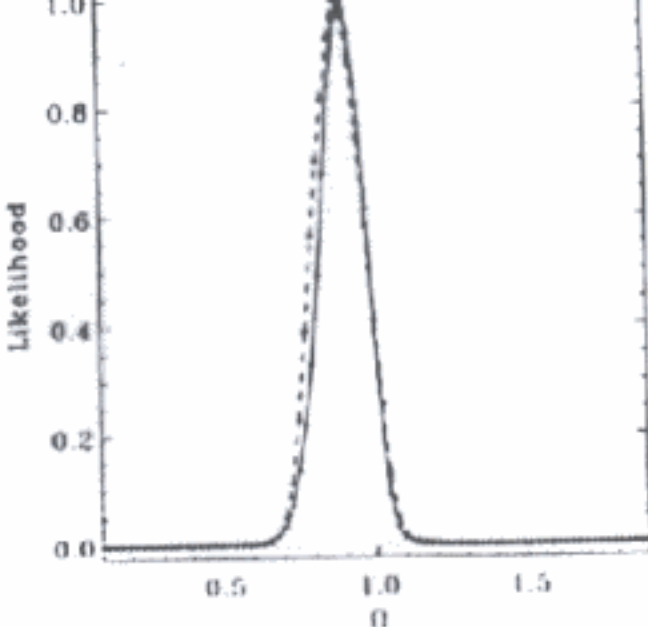
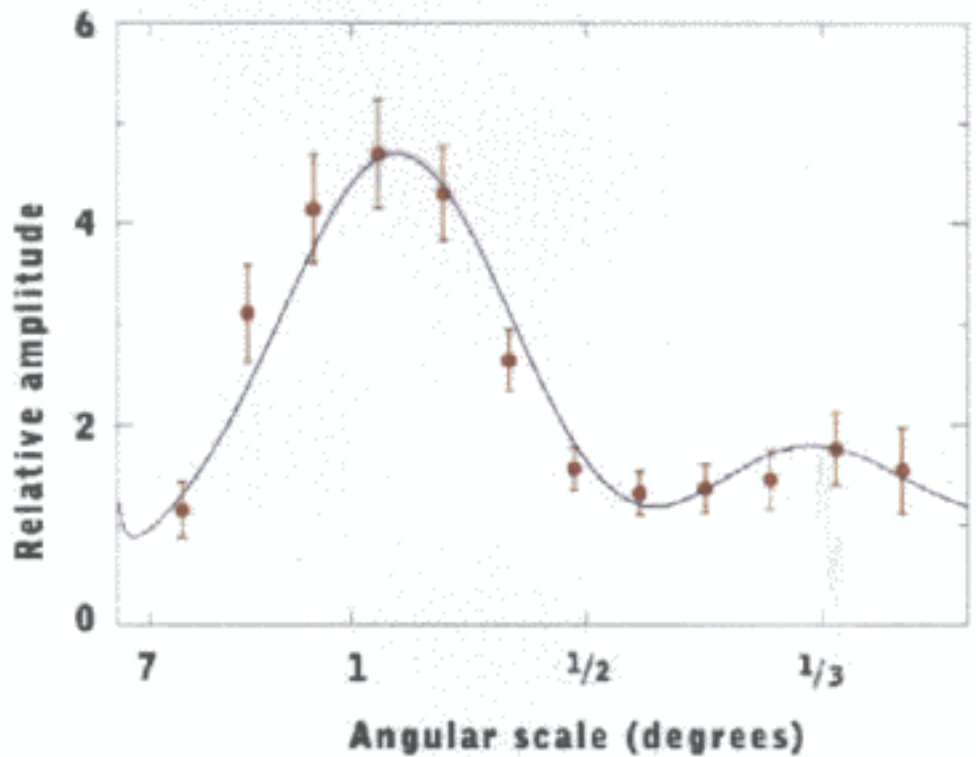


FIG. 1.— Likelihood function of the total energy density of the universe  $\Omega$ . The solid line was obtained by maximizing over all other parameters over the ranges described in the text, while the dashed line was obtained by constraining  $\Omega_bh^2 = 0.0190 \pm 0.0024$  and  $H_0 = 65 \pm 7 \text{ km s}^{-1} \text{ Mpc}^{-1}$ . The intersections with the horizontal line give the bounds for 95% confidence.

Figure 1 shows the likelihood of the total energy density of the universe,  $\Omega$ . We obtain the solid line if we maximize over all the remaining parameters; we get the dashed line if we impose the big bang nucleosynthesis (BBN) constraint  $\Omega_bh^2 = 0.0190 \pm 0.0024$  (Tytler et al. 2000), and restrict  $H_0 = 65 \pm 7 \text{ km s}^{-1} \text{ Mpc}^{-1}$  (Freedman 1999). The two likelihoods differ very little. From the solid line we see that  $0.75 < \Omega < 1.05$  at the 95% confidence level.

We identified the other tightly constrained parameters from a principal component analysis of the likelihood function (Efstathiou & Bond 1999). In Figure 2 we plot the likelihoods for three well-constrained parameters, the physical baryon density,  $\Omega_bh^2$ , the physical cold dark matter density,  $\Omega_{cdm}h^2$ , and the spectral index of primordial scalar fluctuations,  $n_s$ . The likelihood for each parameter was obtained by maximizing over all the remaining parameters.



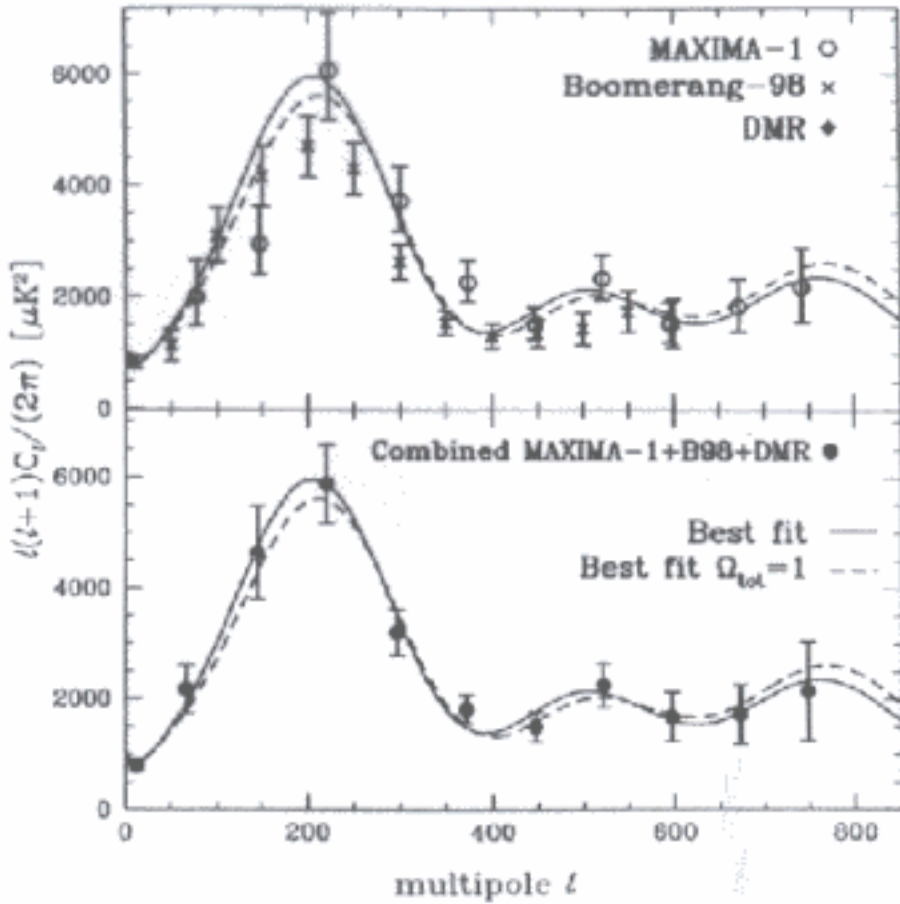


FIG. 1: CMB power spectra,  $C_\ell = \ell(\ell + 1)C_\ell/2\pi$ . Top: MAXIMA-1, B98 and COBE-DMR. Bottom: maximum-likelihood fit to the power in bands for the three spectra, marginalized over beam and calibration uncertainty. In both panels the curves show the best fit model in the joint parameter estimation with weak priors and the best fit with  $\Omega_{\text{tot}} = 1$ . These models have  $\{\Omega_{\text{tot}}, \Omega_A, \Omega_bh^2, \Omega_ch^2, n_s, r_C\} = \{1.2, 0.5, 0.03, 0.12, 0.95, 0\}$ ,  $\{1, 0.7, 0.03, 0.17, 0.975, 0\}$ . They remain the best fits when the large scale structure prior [22] is added, and when the SN prior [20] is added the  $\Omega_{\text{tot}} = 1$  model becomes the best fit in both cases.

Q

# TIME

⇒ STELLAR AGES

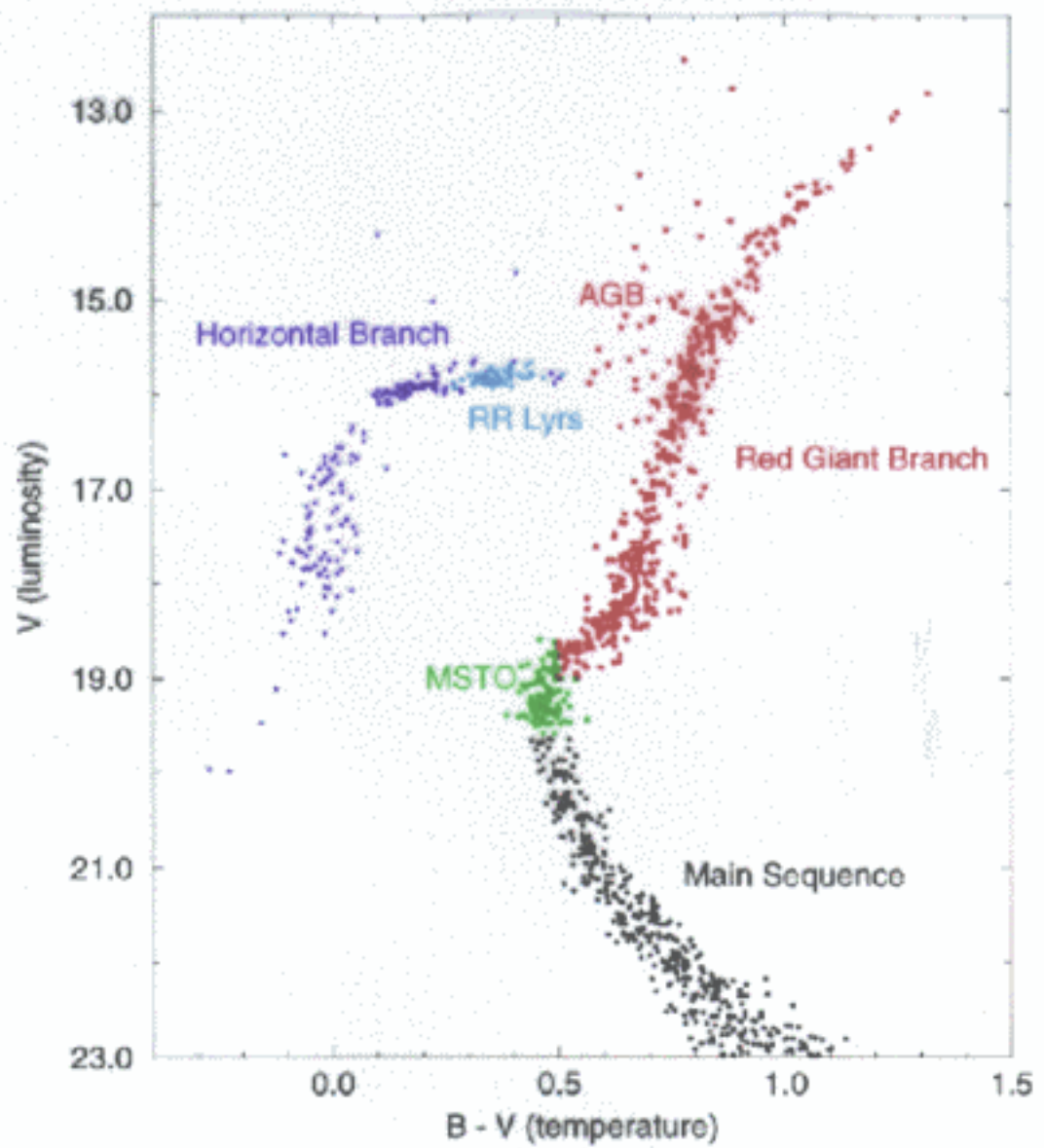
⇒ HUBBLE AGE

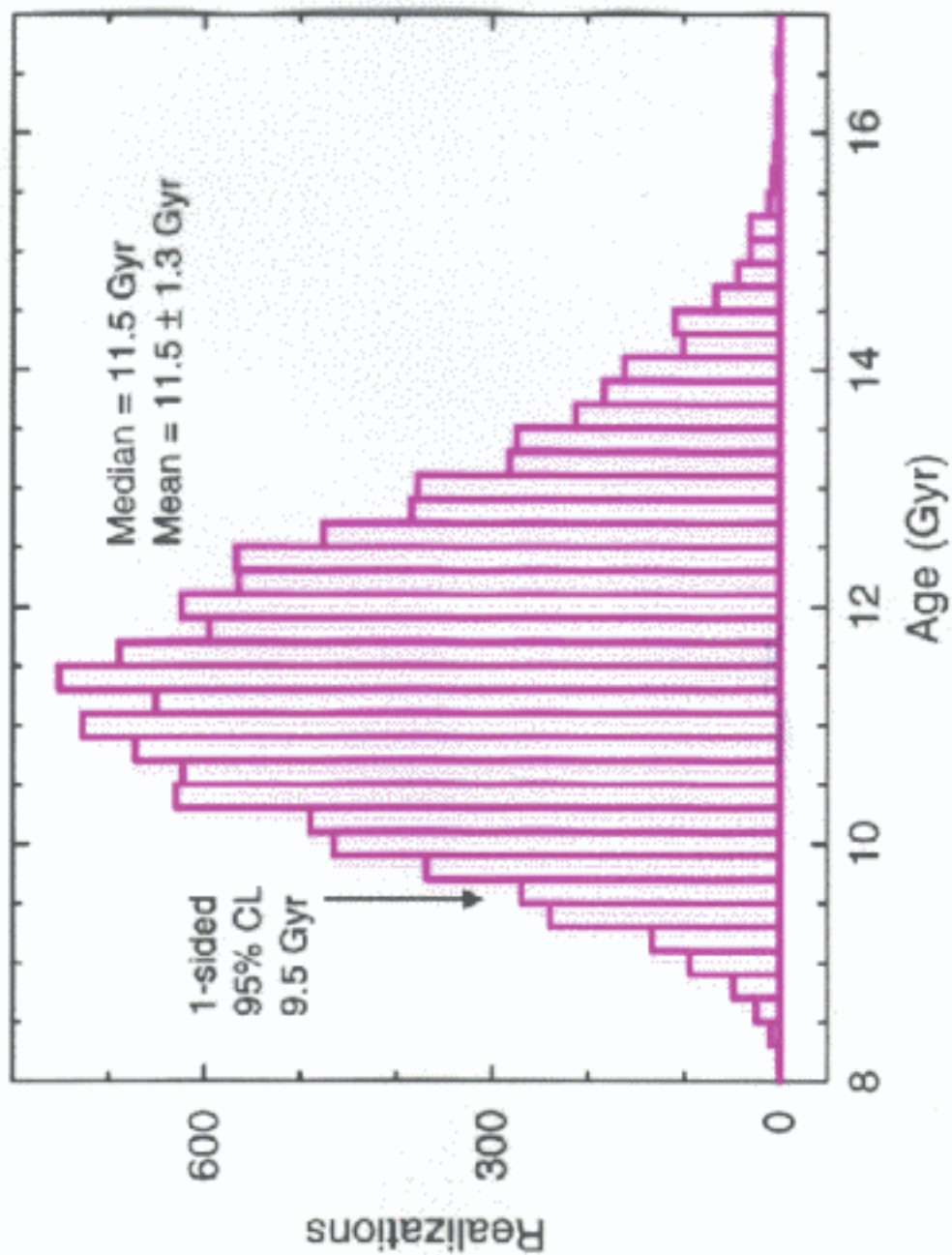
⇒ CONSISTENT EQ. OF STATE

$$\Omega_{\text{TOT}} \simeq 1.1 \pm .12 \quad 95\% \text{ CL}$$

$\Rightarrow$  AN  $\approx$  FLAT UNIVERSE

M15 data from Durrell & Harris (1993)





Age (Gyr) distribution for the simulated data set. The distribution is centered around 11.5 Gyr, with a median of 11.5 Gyr and a mean of  $11.5 \pm 1.3$  Gyr. The 1-sided 95% confidence interval is 9.5 Gyr.

⇒ POSITION OF MSTO ⇒ AGE

⇒ KEY UNCERTAINTY ⇒  $M_V(FR)$

⇒ RR-Lyrae Luminosity

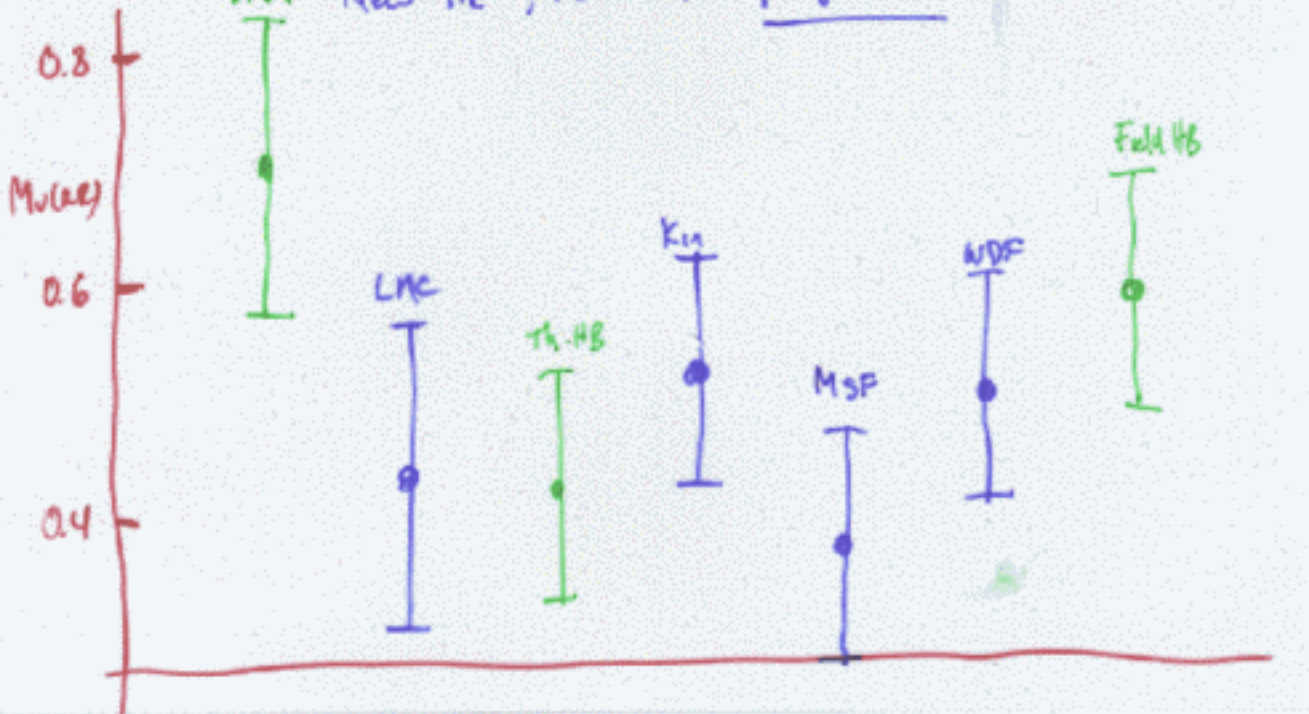
⇒ RR-Lyrae Distance Modulus

B.C., P.O., P.K., L.K. '98 :

$$\boxed{\text{AGE} = 11.5 \pm 1.3 \text{ Gyr } (\pm 2\sigma)}$$

Change : B.C. + LMK '00 :

start New He<sup>+</sup>, rechecks.  $M_V(FR)$



⇒ New Age

$$\approx 12.7 \left\{ \pm \frac{3}{2} \right\} \quad (20)$$

∴ New lower limit  $\sim 11$  Gyr!

Hubble Age:

$H_0 \sim 70 \pm 7$	$\Omega_{\text{TOT}} = 1$	
$\Omega_m$	$\Omega_x$	$t_0$
1	0	$9 \pm 1$ Gyr
0.2	0.8	$15 \pm 1.5$ Gyr
0.3	0.7	$13.5 \pm 1.5$ Gyr
0.35	0.65	$12.7 \pm 1.4$ Gyr

definitely requires  $\Omega_x$  ( $\omega = p/\rho < 0$ )

③

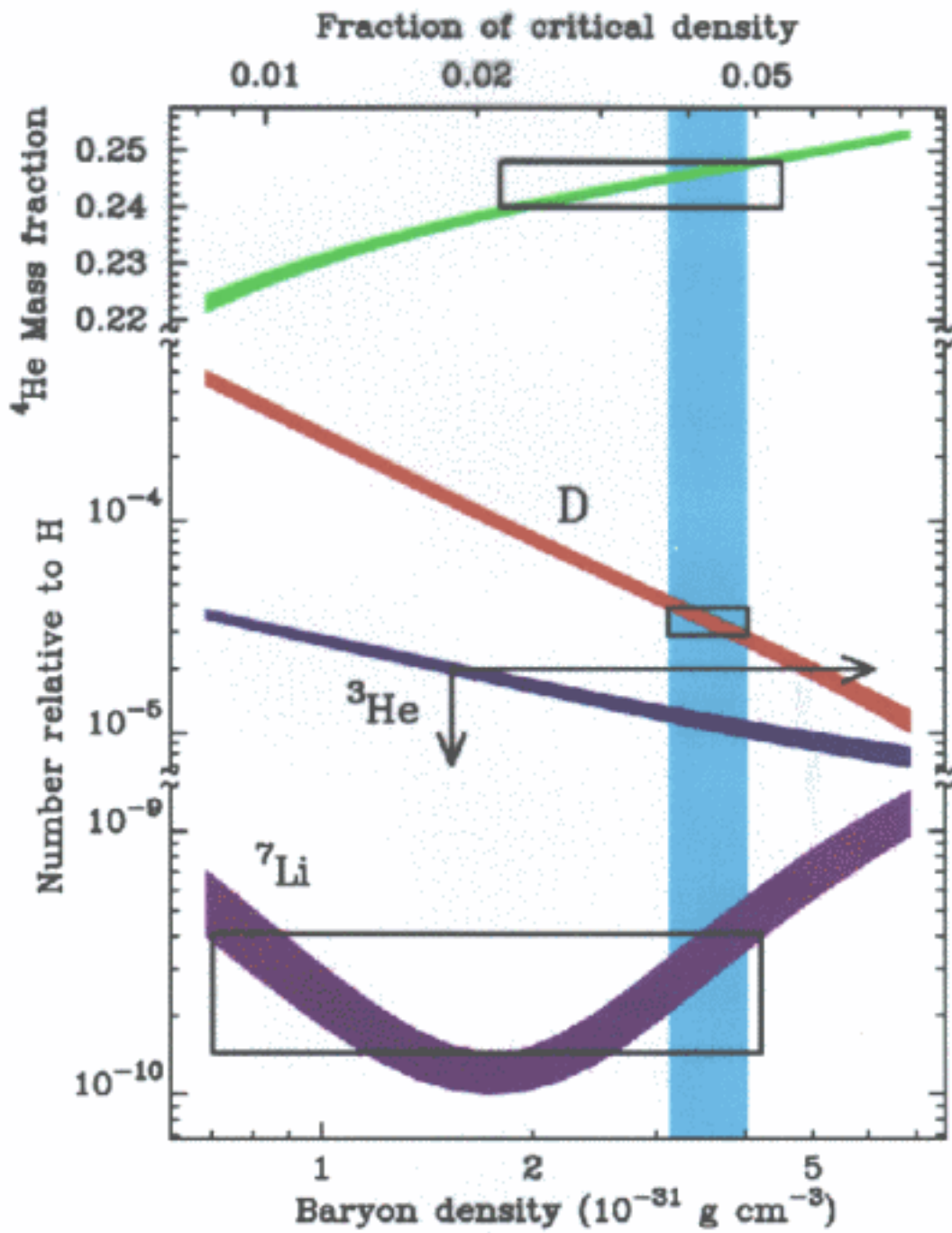
# MATTER

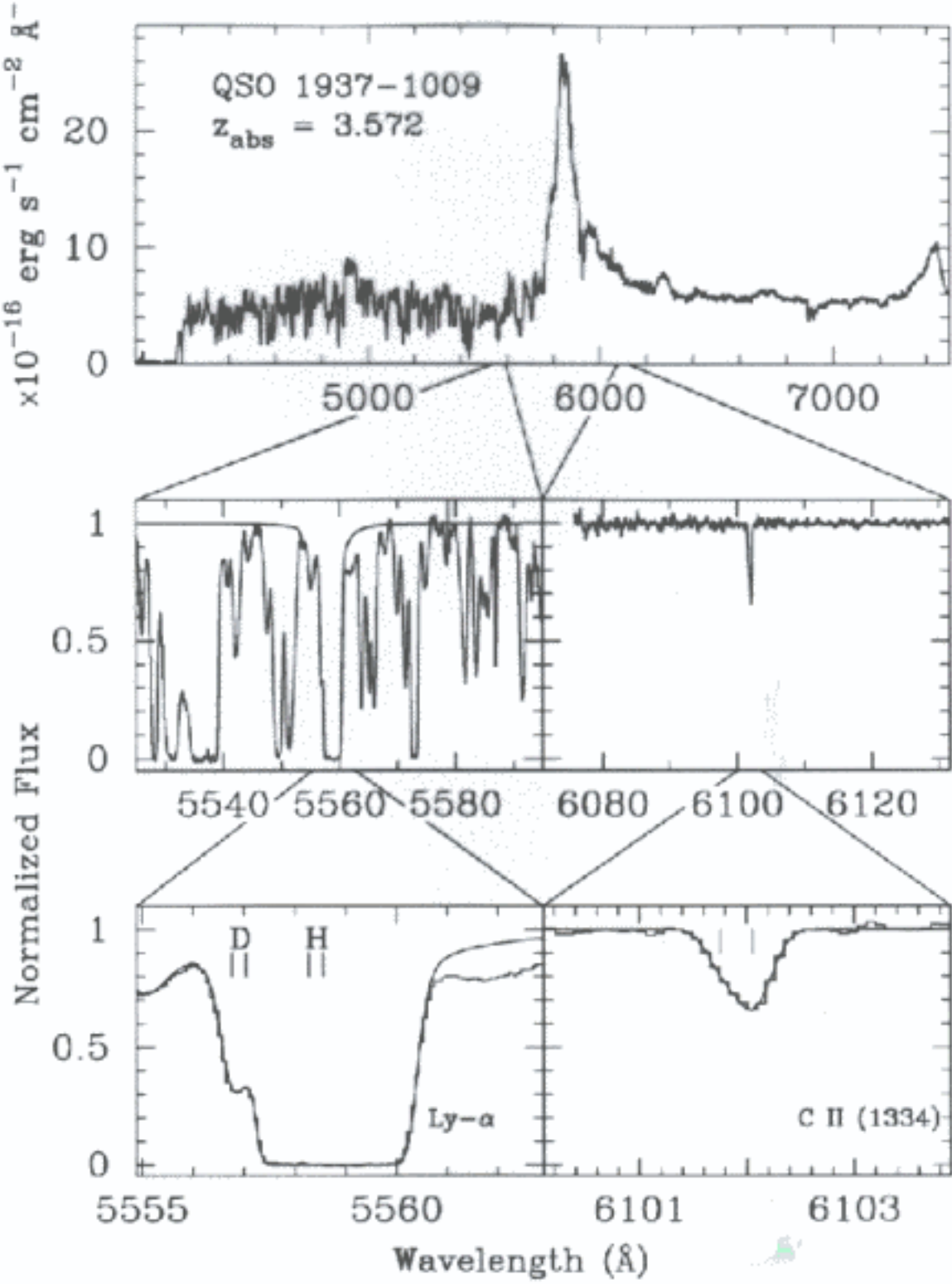
$\Rightarrow \Sigma_B h^2 \Rightarrow$  consistency or crisis?

$\Rightarrow \Sigma_M:$  {  
LSS  
X-Ray  
SZE  
GL  
DN<sub>I</sub>a}

$\Leftarrow$  N.B. D.M.!

$\Rightarrow$  eq. of state.





(i)  $\Omega_B h^2$ :

BBN: Deuterium  $(D/H) = (3.3 \pm 0.5) \times 10^{-5} (2\sigma)$

$$\boxed{\Omega_B h^2 = .0190 \pm .0018 \quad (2\sigma)}$$

$\uparrow$   
(D/H, nucl. reactions?)

$\Rightarrow$  ALL L.E.  $(\Omega_B h^2 = .016 - .025)$  want case

CMB: 2nd peak:

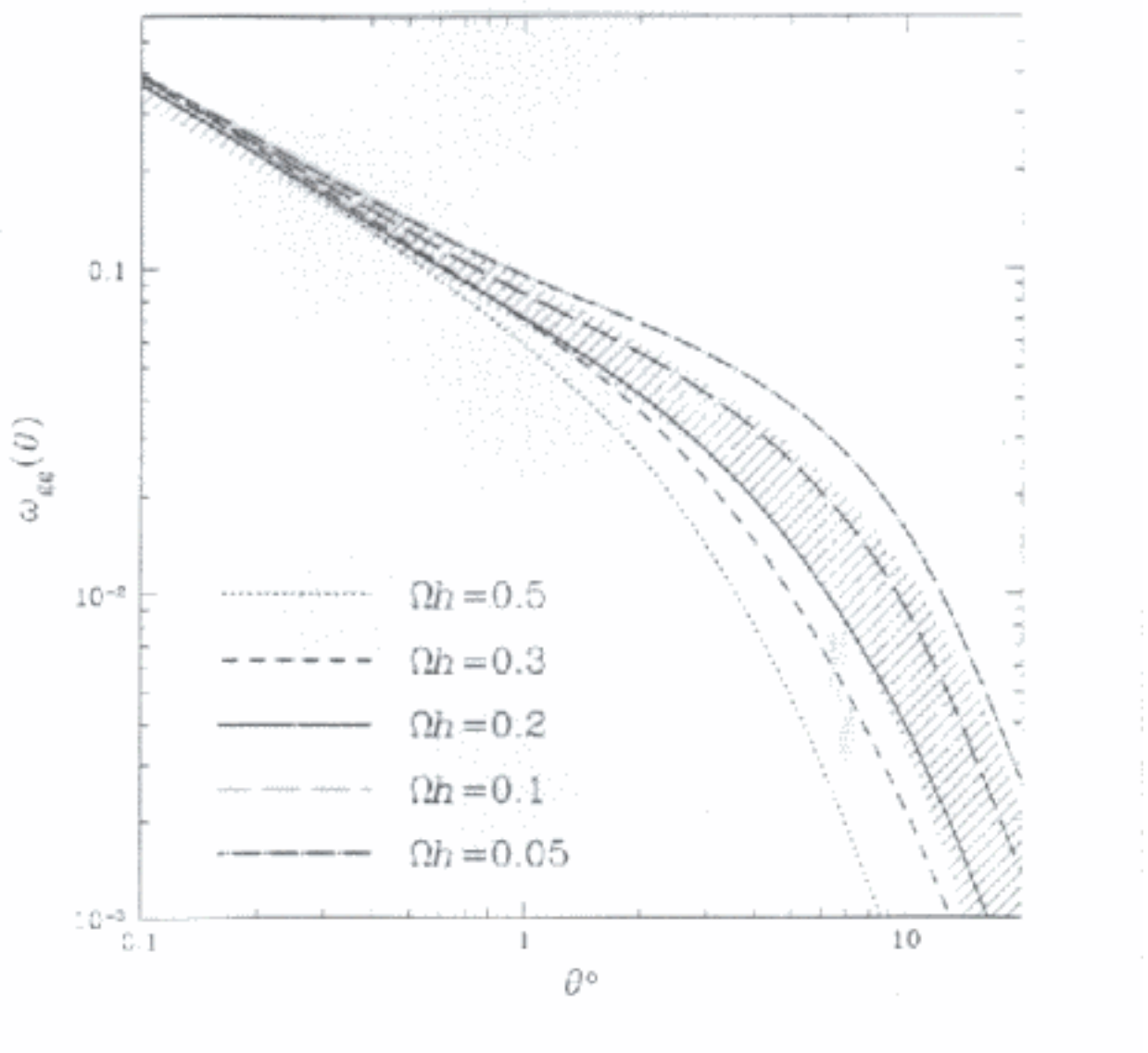
$$\boxed{\Omega_B h^2 = .032 \pm .009 \quad (2\sigma)}$$

Consistency, or Crisis?:

$\Rightarrow$  too early: CMB ... depends on other params,  
early ....

$$\therefore \Omega_B = .03 - .06 = \boxed{.045 \pm .015}$$

Figure 3



$\Omega_M$ :

(a) LSS:  $.25 \leq \Omega_{\text{m}} h \leq .35$

(b) Cluster Evolution:  $\Delta \Omega_m < 0.5$

\* (c) X-RAY CLUSTERS:

(d) X-RAYS: HOT GAS  $T \sim 10^7 \text{ K}$



Hydrostatic Eq:  $(T, R) \rightarrow (M_{\text{gas}}, M_{\text{tot}})$

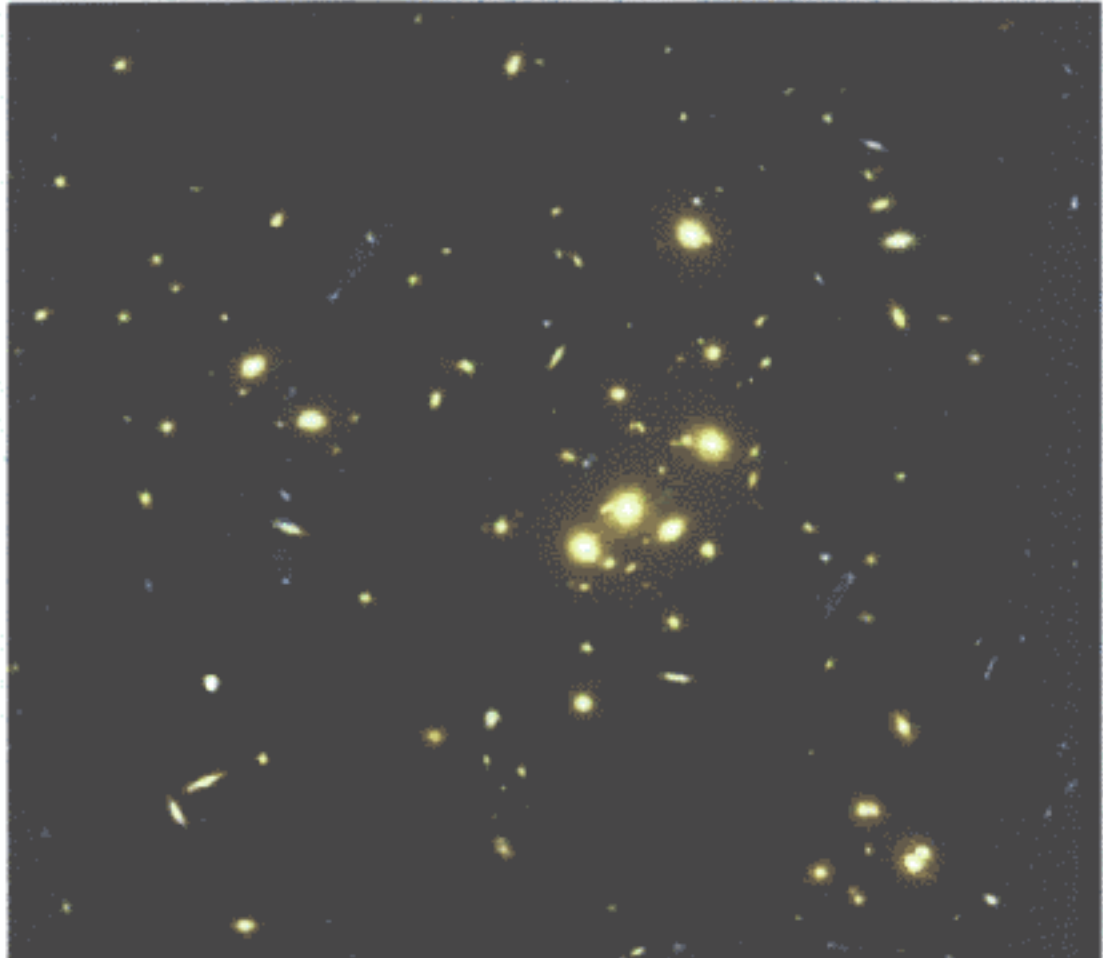
$$f_B = \frac{M_{\text{gas}}}{M_{\text{tot}}} \leq \frac{\Omega_B}{\Omega_M} = (.212 \pm .006) h_{50}^{-5/2}$$

$$\Rightarrow \Omega_m \leq \frac{\Omega_B}{f_B} \approx 0.45 h_{50}^{-1/2}$$

\* (ii) SZE: INDEP EST. OF  $M_{\text{gas}}: \int (n_e) d\ell$   
 $\Rightarrow f_B$ .

$$\Omega_m h_{50} \leq 0.50$$

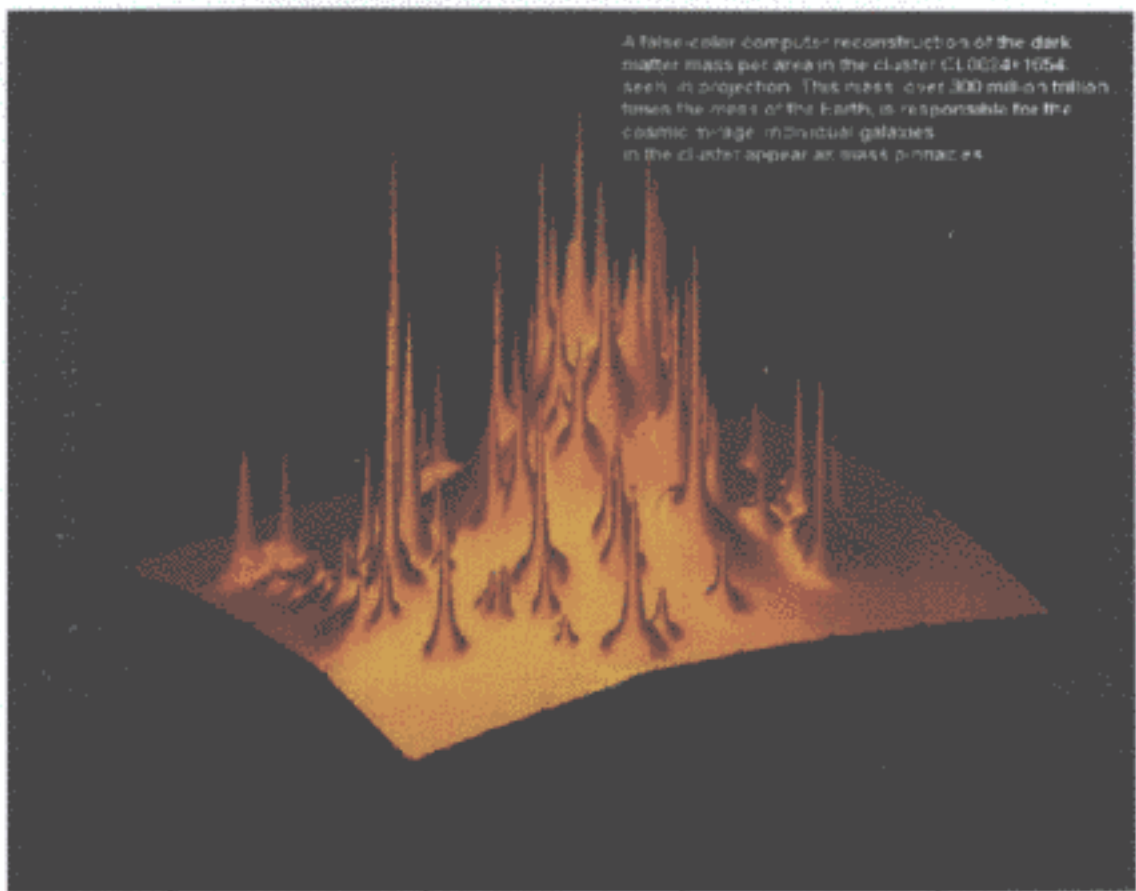
$H = 63-76 \Rightarrow \Omega_m \approx .35 \Rightarrow [DM \neq \text{Baryons}]$



5'

# Galaxy Clusters

Galaxy clusters are the largest structures in the universe. They contain thousands of galaxies and trillions of stars.



The figure shows a false-color computer reconstruction of the dark matter mass per area in the Abell 2029 galaxy cluster.

The reconstruction is based on observations made by the Hubble Space Telescope and the Chandra X-ray Observatory.

The cluster contains over 1000 galaxies and has a total mass of approximately 10<sup>14.5</sup> solar masses.

The cluster is located at a distance of about 400 million light years from Earth.

The cluster is part of the Virgo Supercluster, one of the largest known structures in the universe.

The cluster is also associated with a strong X-ray emission, which is used to study the properties of the cluster's gas.

The cluster is an important object for studying the evolution of structure in the universe and the properties of dark matter.

The cluster is also an important object for studying the evolution of structure in the universe and the properties of dark matter.

No Bahcall et al. '92

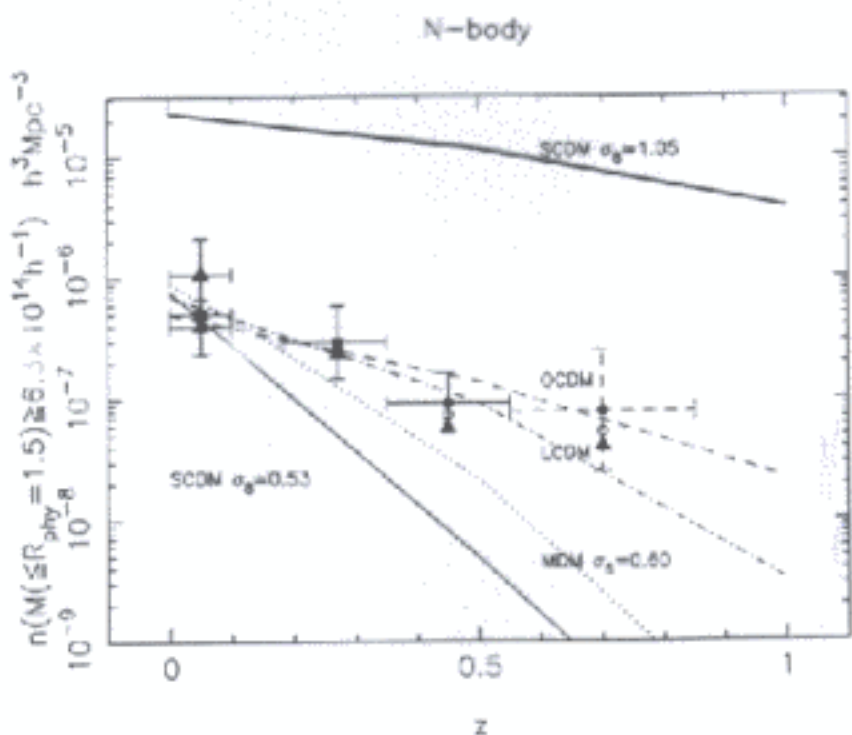


Fig. 2 The evolution of cluster abundance with redshift for massive, coma-like clusters ( $M_{1.5} \geq 6.3 \times 10^{14} h^{-1} M_\odot$ ). The lines represent model predictions; the data points are from the CNOC survey. From Bahcall, Fan and Cen (1997) (updated fig.).

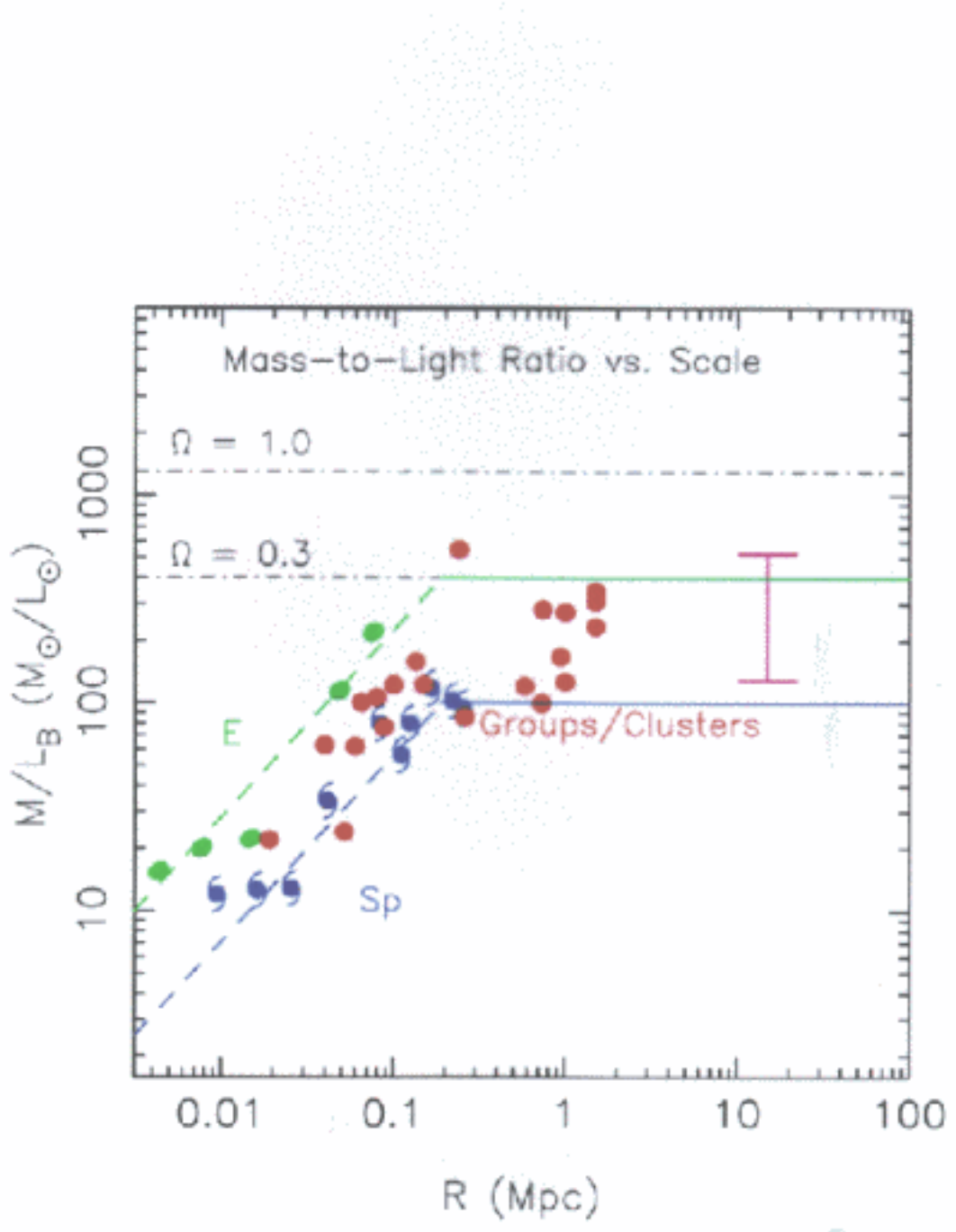




Figure 1. A photograph of a man with a mustache and a goatee. The image is used to illustrate the concept of facial hair in the study.

the subjects were asked to respond to a series of questions about their attitudes towards the man in the photograph. Specifically, they were asked to indicate whether they found him attractive or unattractive, and whether they would be willing to date him.

The results showed that the subjects found the man with facial hair more attractive than the man without facial hair, and were more willing to date him. This suggests that facial hair may have a positive effect on perceived attractiveness.

It is important to note that this study only examined the effect of facial hair on perceived attractiveness. It did not examine other factors that may also contribute to perceived attractiveness, such as physical fitness or social status.

Overall, the results suggest that facial hair may have a positive effect on perceived attractiveness. However, it is important to remember that this is just one factor among many that contribute to perceived attractiveness.

In conclusion, the results of this study support the hypothesis that facial hair may have a positive effect on perceived attractiveness. However, it is important to remember that this is just one factor among many that contribute to perceived attractiveness.

References:

1. *Journal of Nonverbal Behavior*, 1980, 14, 111-125.

2. *Journal of Nonverbal Behavior*, 1980, 14, 111-125.

3. *Journal of Nonverbal Behavior*, 1980, 14, 111-125.

4. *Journal of Nonverbal Behavior*, 1980, 14, 111-125.

5. *Journal of Nonverbal Behavior*, 1980, 14, 111-125.

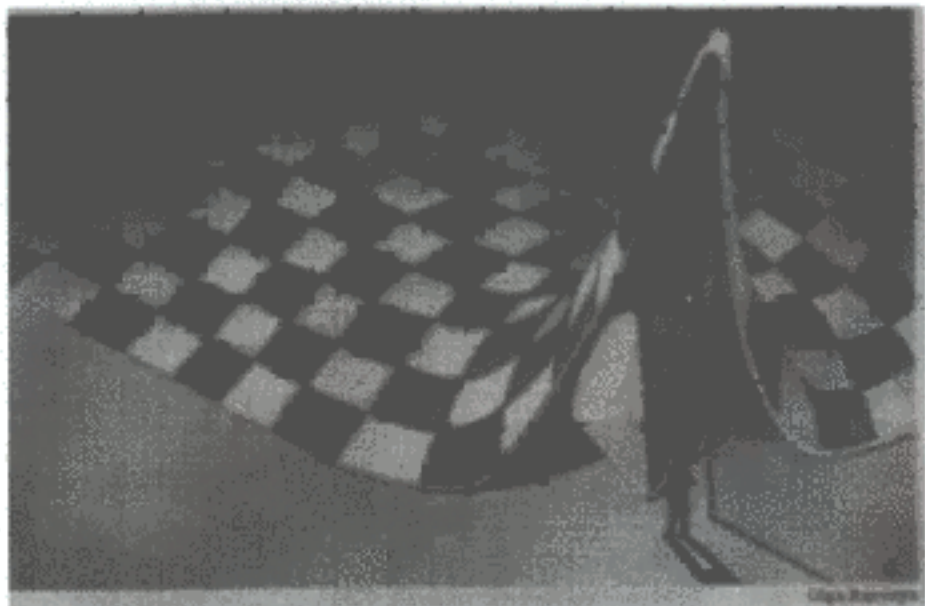


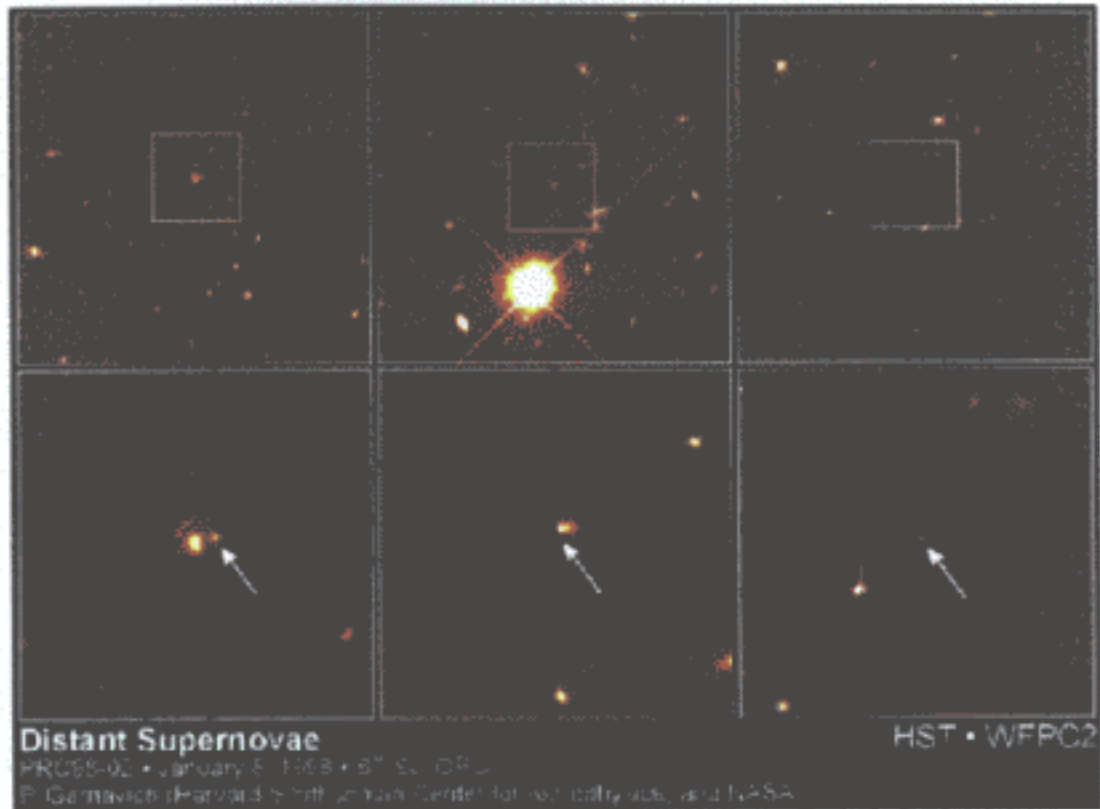
Fig. 1. A woman wearing a traditional sash (Photo: M. Saito).

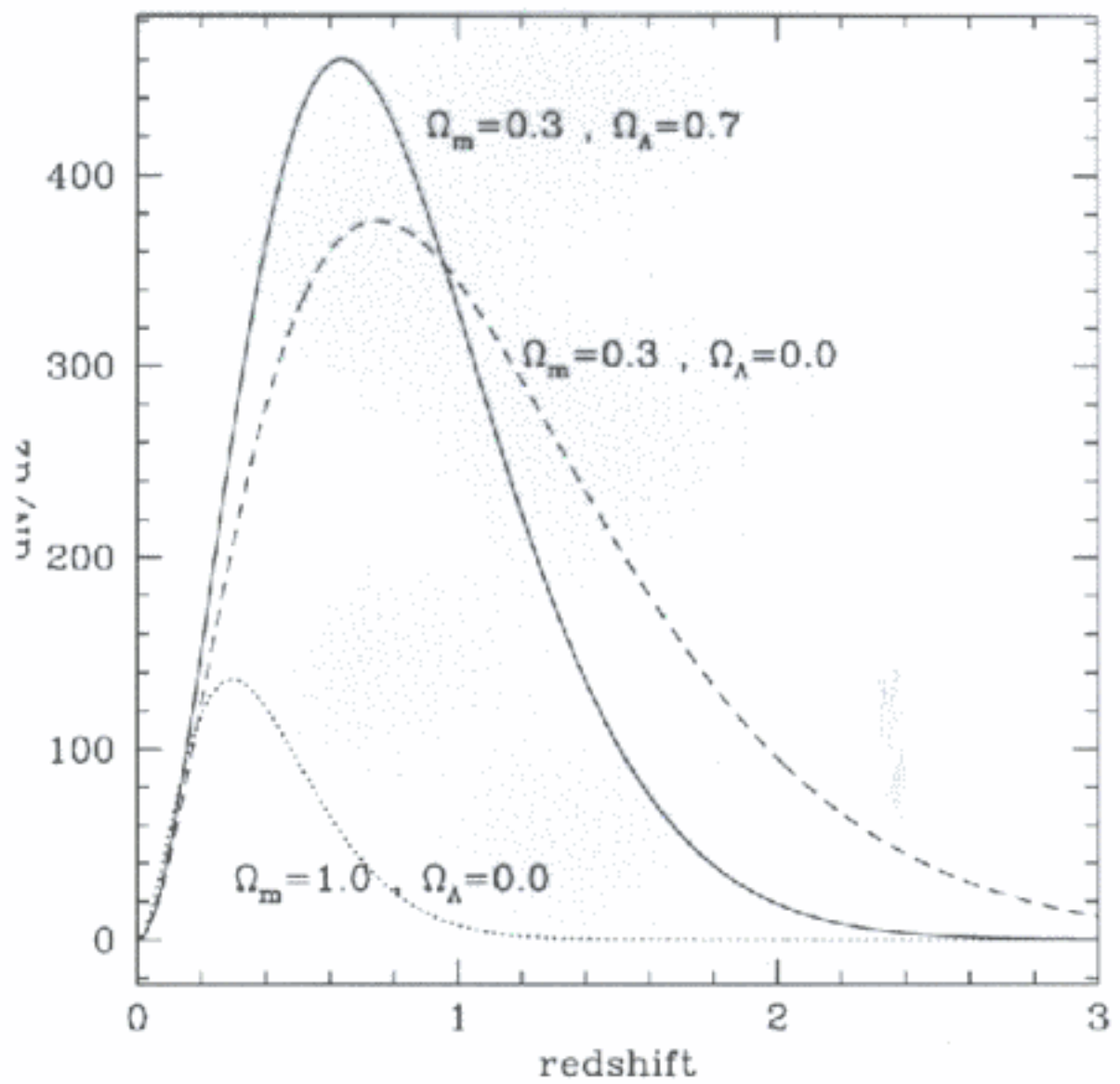


Fig. 2. A woman wearing a traditional sash (Photo: M. Saito).

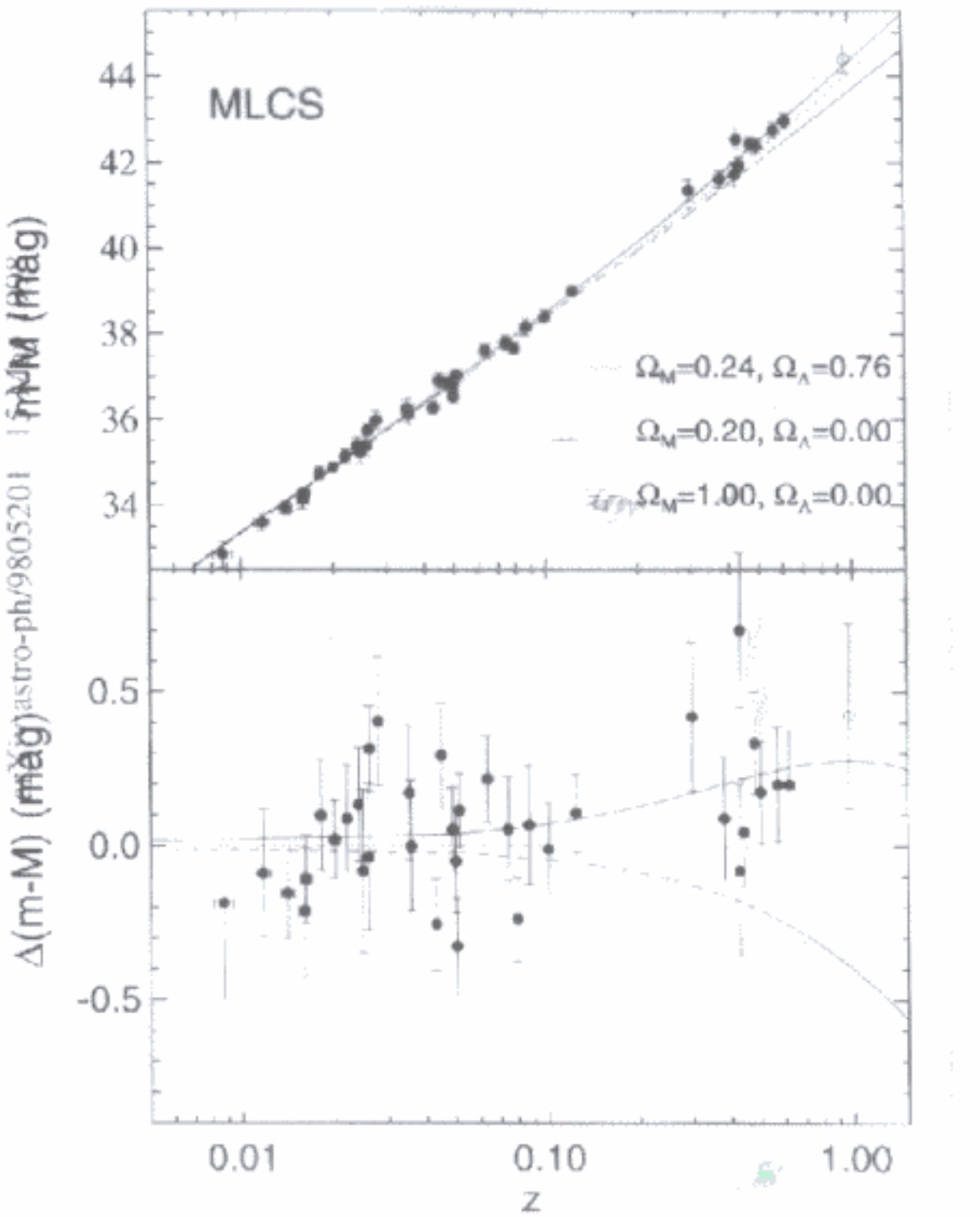


Fig. 3. A woman wearing a traditional sash (Photo: M. Saito).





The Future: Clusters : size,



$$\left( \begin{array}{c} \rho \\ p \end{array} \right) = \left\{ \begin{array}{ll} 0 & \text{red} \\ 1 & \text{green} \\ -1 & \text{blue} \end{array} \right\}$$

## DARK ENERGY $\{ -1 \leq w \leq 0 \}$

"QUINTESSENCE"

$w \rightarrow$  evolves ...



"TRACKER"

$w \geq -0.6$

LIMITS : SNIA :

$$w \leq -0.6$$

HOW WELL?

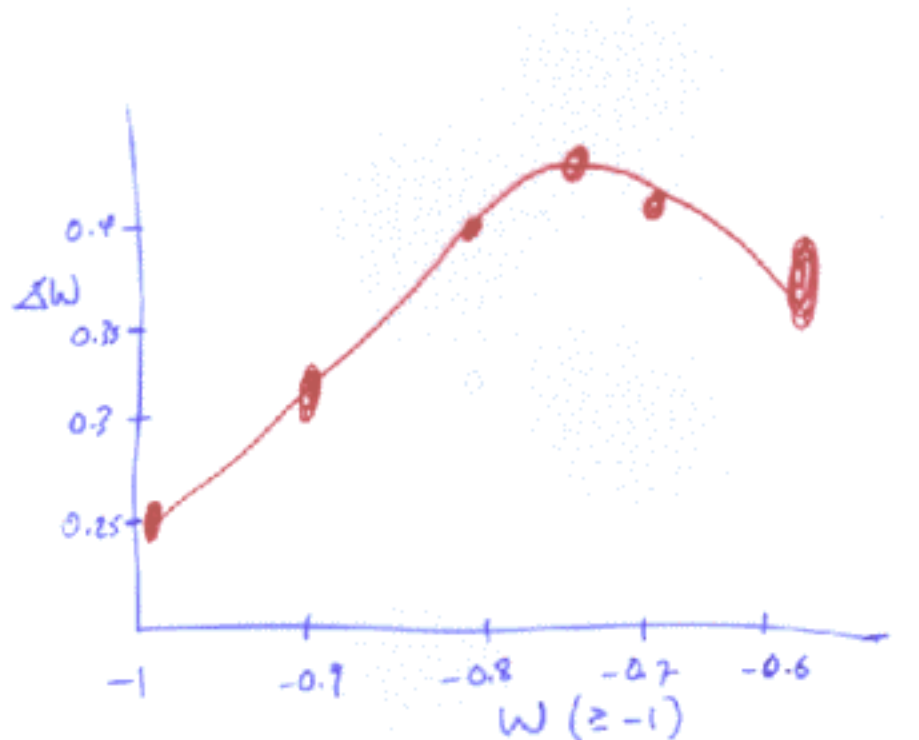
$$w \leq -0.7$$

$$100 \text{ SN}$$

$z \sim 0.5 - 1.5$   
(LWK, CD '00)

$\Delta w \sim 10\%$  200 SN spec ?

$\Delta w \sim 10\%$  Galaxy evolution ?  
(2w)



LHK, EL, CD

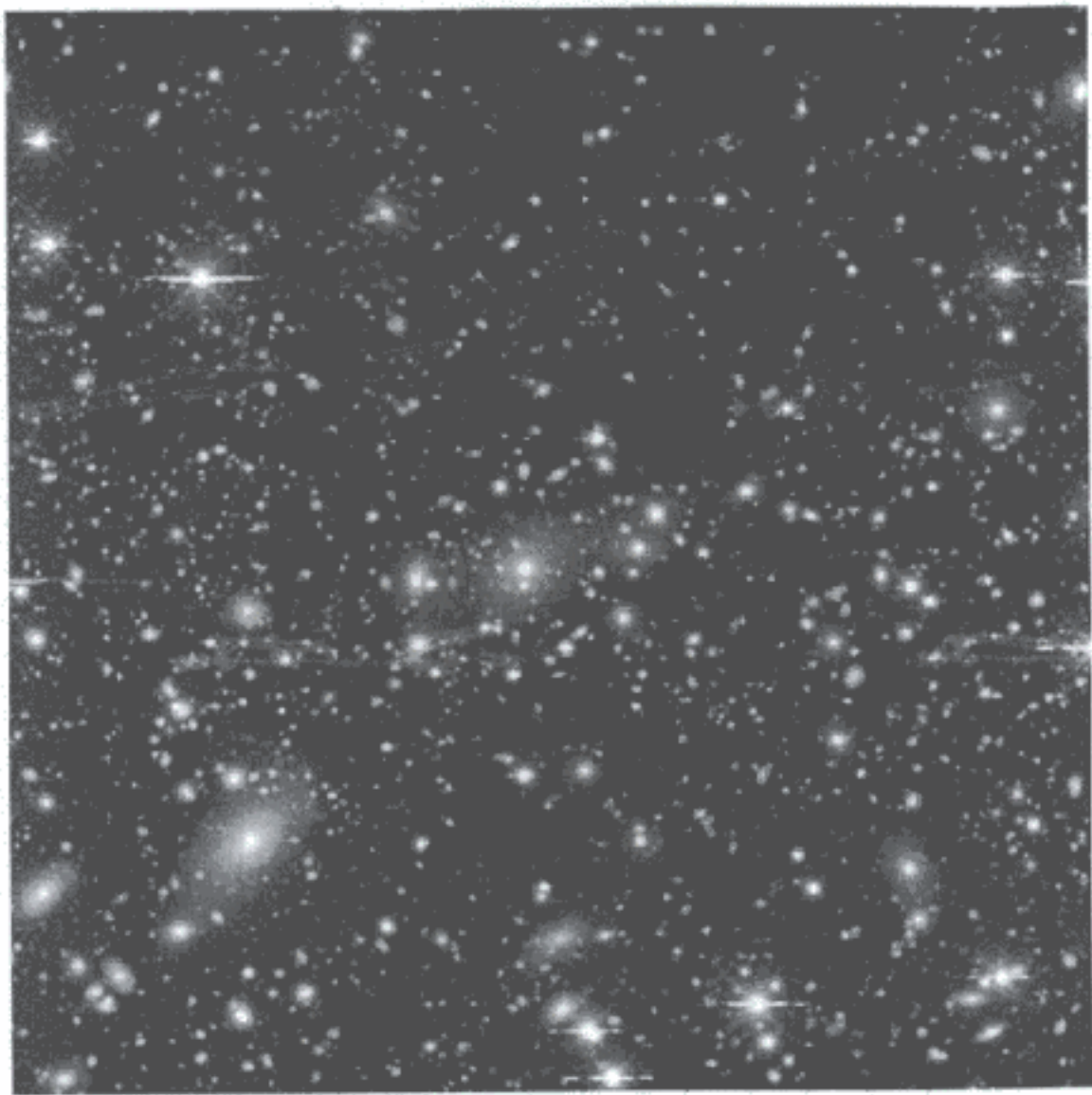
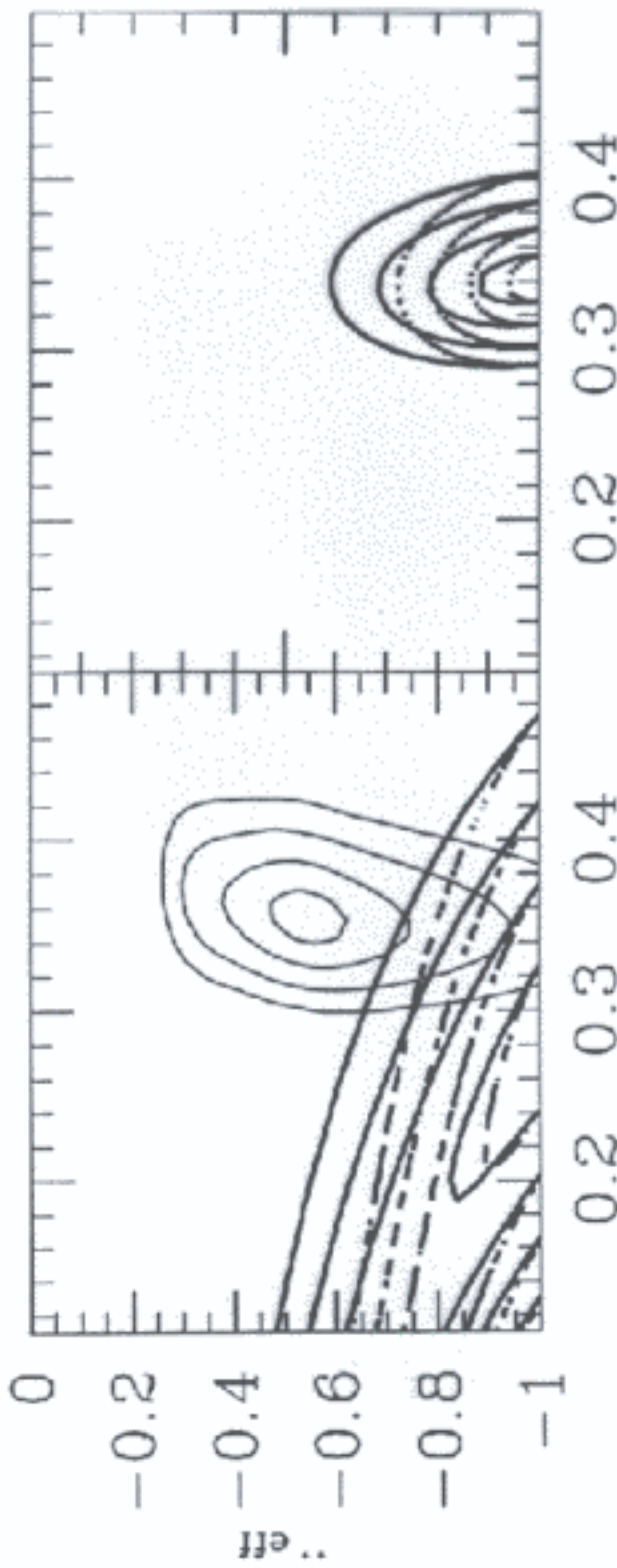


Figure 1. A dense cluster of stars against a dark background. The stars vary in brightness and color, with many appearing as small white or yellow points of light. A few larger, more luminous stars are visible, particularly towards the bottom left and center. The background is a deep black, indicating the vastness of space.

The image is a square frame with a resolution of approximately 1000x1000 pixels. The stars are distributed throughout the frame, with a higher density in the center and a gradual decrease towards the edges.

### III. RESULTS



contours of likelihood, from  $0.5\sigma$  to  $2\sigma$ , in the  $\Omega_M$ - $w_{\text{eff}}$  plane. Left: The thin solid lines are the constraints from the CMB. The heavy lines are the SN Ia constraints (using the Fit C supernovae of Ref. [1]) for constant  $w$  (solid curves; quadratic and quartic potentials) and for a scalar-field model with an exponential potential (broken curves; quadratic and quartic potentials). Note that the SN Ia contours for dynamical scalar-field models and constant  $w$  are very similar (see text). Right: The likelihood contours from all of our cosmological constraints for constant  $w$  model scalar-field models (broken).

## CONCLUSIONS:

IT DOESN'T REALLY MATTER:

NO SET OF MEASUREMENTS OF  
COSMOLOGICAL PARAMETERS  
WILL EVER ALLOW A  
DETERMINATION OF THE  
ULTIMATE DESTINY OF THE  
UNIVERSE!

LAR + MST